Clim. Past Discuss., 5, 287–326, 2009
www.clim-past-discuss.net/5/287/2009/

Climate of the Past Discussions

Climate of the Past Discussions is the access reviewed discussion forum of *Climate of the Past*

Mid-Holocene regional reorganization of climate variability

K. W. Wirtz[1], K. Bernhardt[1,2], G. Lohmann[3], and C. Lemmen[1]

[1]GKSS Research Center Geesthacht, Institute for Coastal Research, Max-Planck Straße 1, 21501 Geesthacht, Germany
[2]Carl-von-Ossietzky Universität Oldenburg, Institute for Chemistry and Biology of the Marine Environment (ICBM), Carl-von-Ossietzky Straße, 26111 Oldenburg, Germany
[3]Alfred Wegener Institute for Polar and Marine Research, P.O. Box 180, 27483 Bremerhaven, Germany

Received: 12 December 2008 – Accepted: 12 December 2008 – Published: 28 January 2009

Correspondence to: K. W. Wirtz (wirtz@gkss.de)

Published by Copernicus Publications on behalf of the European Geosciences Union.

Abstract

We integrate 130 globally distributed proxy time series to refine the understanding of climate variability during the Holocene. Cyclic anomalies and temporal trends in periodicity from the Lower to the Upper Holocene are extracted by combining Lomb-Scargle Fourier-transformed spectra with bootstrapping. Results were cross-checked by counting events in the time series. Main outcomes are: First, the propensity of the climate system to fluctuations is a region specific property. Many records of adjacent sites reveal a similar change in variability although they belong to different proxy types (e.g., δ^{18}O, lithic composition). Secondly, at most sites, irreversible change occured in the Mid-Holocene. We suggest that altered ocean circulation together with slightly modified coupling intensity between regional climate subsystems around the 5.5 kyr BP event (termination of the African Humid Period) were responsible for the shift. Fluctuations especially intensified along a pan-American corridor. This may have led to an unequal crisis probability for early human civilizations in the Old and New World. Our study did not produce evidence for millennial scale cyclicity in some solar activity proxies for the Upper Holocene, nor for a privileged role of the prominent 250, 550, 900 and 1450 yr cycles. This lack of global periodicities corroborates the regional character of climate variability.

1 Introduction

There was hardly any period in Earth's history that experienced more stability in the climate system than did the Holocene. According to Richerson et al. (2001), even the onset of human civilizations is owed to the lack of large climate fluctuations, since change was the constant rule for all preceding glacial as well as interglacial periods within the Quaternary. The notion of a stable Holocene climate has been, meanwhile, questioned by many researchers (e.g. Fairbridge and Hillaire-Marcel, 1977; Bond et al., 1997c; Mayewski et al., 2004). Refined accuracy of paleorecords and of noise reduc-

tion methods has disclosed a series of distinct shifts from most proxies for the last 11,500 years (Barber et al., 2004; Kim et al., 2007). These shifts attract further attention for at least four reasons.

1. Disruptions have – with the exceptions of the Saharan desertification at 5500 yr BP (Claussen et al., 1999) and the 8.2 kyr event (Renssen et al., 2001) – not yet been reproduced by numerical modeling. Mechanistic understanding of the complex interplay between ice, ocean, atmosphere and vegetation bundled in regional climate sub-systems is far from being complete (Steig, 1999).

2. We also still lack knowledge about the spatial extension of prominent disruptions (deMenocal et al., 2000b; Sirocko, 2003; Mayewski et al., 2004). So far, only the work of Rimbu et al. (2004) based on 18 records of alkenone sea surface temperature worldwide revealed consistent regional differences of climate variability.

3. Holocene climate fluctuations define the range of natural variability to which the signatures of anthropogenic interference with the Earth system should be compared (von Storch et al., 2004; Moberg et al., 2005). Attribution and analysis of past shifts is pivotal for assessing ongoing changes, as well as reproduction of recorded natural variability (of the Holocene) by models is a prerequisite for simulating future climates (in the Anthropocene).

4. Another motivation to seek for past, but not too remote alterations, especially in regional temperature or moisture is the "breeding" role of the Holocene for civilizations. While its stability has been claimed to be responsible for their rising, instabilities are first candidates for explaining their collapses. This idea is reflected by numerous studies where individual outbreaks in proxy time series have been correlated with eclipses of ancient empires (Fagan, 1999; Anderson, 2001; deMenocal, 2001; Binford, 2001). Provoked by the simplicity of this approach, a large group of historical scientists dislike such intrusion by geoscience into their discipline (Erickson, 1999; Coombes and Barber, 2005).

Fragmented (model) knowledge and controversy are hence characterizing both the effects as well as causes of singular Holocene climate shifts. Evidence for the nearly regular cyclicity of events, however, seems to be firm. Predominant modes of punctuated disruptions on millennial time scales have since long been identified (e.g. Fairbridge and Hillaire-Marcel, 1977). For the North Atlantic, the 1450 yr periodicity was proposed by Bond et al. (1997c), and is relevant in tropical regions as well (deMenocal et al., 2000b; Thompson et al., 2003b). On the centennial time scale, recurrent climate anomalies were detected by McDermott et al. (2001) or Sarnthein et al. (2003b). Often, an external trigger was suspected behind the quasi-cyclicity – above all variations of solar activity (e.g., Hodell et al., 2001c; Bond et al., 2001c).

Spectral analysis can indicate system properties of the global climate (like stability, turn-over times, regularity of modes) and helps to identify active teleconnections which are generated by the coupling of sub-systems and their feed-backs. If extended to external forcings, analysis in the frequency domain will shed light on the possible origin of shifts. Sensitivity to variable forcing can, for example, be estimated using the quantitative relationship of spectral intensities (Debret et al., 2007). We here provide such a reconstruction of the spectral behavior inherent to climate proxy time series with global coverage and for the entire Holocene. Former data reviews were mostly centered around an eventual synchronicity or spatial intensity of shifts (e.g. Mayewski et al., 2004; Seppä et al., 2007), while spectral synthesis studies cover either a single climate zone or a shorter interval within the Holocene (e.g. Morrill et al., 2003; Moberg et al., 2005).

Here, a spectral analysis technique is introduced that is adapted to unravel the temporal wax and wane of dominant fluctuation modes. Operating with this tool on a global set of proxy time series, we not only aim to address the question of how quasi-cyclic modes were distributed worldwide and which factors could be tentatively claimed being responsible for them. Acknowledging the observation that millennial as well as centennial modes are discontinuous or even missing in a number of high-resolution records (e.g. Noren et al., 2002b; Moberg et al., 2005), our study focuses on temporal and spa-

tial trends in the intensity of climate fluctuation modes. The study of variability trends in time and space reflects in particular the questions: Has the climate system of the Holocene continuously stayed in a unique state? Does its stability (*sensu* retaining of large shifts) as well as instability (disposition to minor fluctuations) reflect a global property or distinct regional features?

2 Selection of proxy data

In total 130 long-term high-resolution time series obtained at 109 globally distributed sites were collected from existing literature. Due to low sedimentation rate resulting in coarse temporal resolution, open ocean locations are underrepresented with respect to coasts and land masses (Fig. 1). 77% of the records have temporal resolution better than 100 yr and 80% span more than 9000 yr within the period 12 kyr BP to the present (see Table 1 and 2). 68 data sets are accessible from one of the Publishing Network for Geoscientific & Environmental Data (PANGEA, www.pangea.de) or the National Climate Data Center (NOAA NCDC, www.ncdc.noaa.gov). The remaining time series were digitized with an error of less than 2% from original publications .

We chose to analyze time series based on quantities that serve as proxies for temperature, effective moisture (i.e. precipitation – evaporation), and rarely also wind regime, not unlike Mayewski et al. (2004). Records were excluded which involve more complex relationships to climate, such as productivity or stable carbon isotopes. The types of records are broadly categorized in Table 1 into (1) isotope fractionation, mostly δ^{18}O, (2) lithic composition, and (3) relative species abundance (tree pollen or algae). In addition, solar activity was inferred from ^{10}Be abundance and ^{14}C flux (Bond et al., 2001c).

2.1 Lomb-Scargle spectral analysis

We employ a spectral analysis since this approach is not sensitive against possible absolute dating errors. Spectral information can be interpreted independently from the different and sometimes uncertain correlations of individual variables with the climate state (like for isotope fractionation in ice cores, lake or marine sediments, or pollen composition) what allows to use a broader spectrum of proxy types. If one is in particular interested in the temporal change of power spectra, wavelet transformation is usually the method of choice (Moy et al., 2002; Moberg et al., 2005). However, wavelets require evenly sampled time-series, while time sequences of proxy records are mostly irregular. To avoid the introduction of a spectral bias by interpolation and, in addition, to make the method also applicable to records with relatively few samples, we base our approach on the procedure suggested by Schulz and Mudelsee (2002).

This means to employ a Lomb-Scargle Fourier transform followed by a bias correction with correction factor obtained from a theoretical red-noise spectrum which, in turn, is rooted on a Monte-Carlo ensemble of 1000 first order autoregressive processes. We use version 3.5 of the software package REDFIT (www.ncdc.noaa.gov/paleo/softlib/redfit/redfit.html) with parameters ofac=4, hifac=0 and two Welch windows with an overlap of 50%, and assume a 95% confidence level for identifying significant spectral anomalies. For time series with a small fraction (n) of data points in each Welch window, we follow the recommendation by Thomson (1990) and take $1-1/n$ as the threshold for significance.

Acknowledging the notion of a globally visible Mid-Holocene climatic change (e.g. Steig, 1999; Morrill et al., 2003) we split the time series into two overlapping intervals; these intervals (12–5.5 kyr BP and 6.5–0 kyr BP) will be referred to as Lower and Upper Holocene, respectively. The initial age 12kyr BP compromises between the different starting points of the time-series which in some cases reflect the globally asynchronous onset of the Holocene. The exact choice of the starting age, however, was not found to be critical for our analysis.

In order to diagnose the change in spectral intensity from Lower to Upper Holocene we employ a selective bootstrap. Randomly chosen data points were substituted with also randomly chosen values from the same part (Lower/Upper Holocene). Subsequently, the spectrum is examined for changes in significance. We obtained good results for 5000 realizations with substitution fraction of 33% for each time series. From this we statistically identified local long-term changes in the variability signal. Either for the entire spectrum or for a frequency window we checked whether its spectral significance is sensitive to bootstrapping. If a mode looses significance by bootstrapping in the upper interval, but endures changes in the lower part, this corresponds to a positive change in cyclicity (periodic signal originates from the Upper Holocene part of the time-series). The opposite behavior (sensitivity in bootstrapping the lower and robustness in the upper time interval) is attributed to a negative temporal trend.

Spatial clustering of locations is performed by radially extrapolating the peak intensity I from each record location with exponential decrease ($I \cdot \exp(-r/1500\,\mathrm{km})$). Peak intensity is a binary measure with $I=1$ if at site i the sum of all available local proxy information significantly indicates the presence/increase of frequencies, and $I=-1$ for negative trends.

2.2 Non-cyclic event frequency

The analysis in the frequency domain is cross-checked by a simple counting method relying on a straightforward definition of climate events. After removal of the 2 kyr running mean, the time series are normalized by their standard deviation. Frequency peaks are considered as a distinct event if (1) they exceed a threshold p_a and (2) are separated by a zero-line crossing to the preceding event. By using in parallel a vector of thresholds $p_a = 1.5^{-1,0,1,2}$ the method is made robust with respect to the choice of p_a. The non-cyclic event frequency is calculated as the average number of events for different thresholds p_a, divided by the length of the time period.

3 Results

3.1 Mid-Holocene change in climate modes

The way how changes in the spectral intensity are detected by our method is visualized in Fig. 2 for three selected records, i.e. temperature reconstruction for Southeast Europe, δ^{18}O at Sajama, Bolivia, and solar activity from Greenland ice cores. Only those frequency peaks that are with 95% probability not compatible with red noise mark a significant mode. Random displacement of proxy values in one half of the Holocene dampens some of those modes, as, for example, obvious for the 1/340 yr cycles in Southeast Europe temperature during the Upper Holocene. For isotopic oxygen at Sajama, spectral changes are manifold. The 1/900 yr mode vanishes when either of the two halves is distorted by bootstrapping, and the two prominent centennial cycles (1/250 yr, 1/200 yr) appear in the Upper Holocene only. In this period, the well known 1000 yr mode of solar activity turns out to be absent. Just by visual inspection, one could suspect its presence in the Lower Holocene according to the relatively high spectral intensity, the value of which, however, is below the critical threshold for significance.

Apart from the three example records, we detected in all 130 time series 223 significant modes in the spectral interval between 1/200 yr and 1/1800 yr (see also Fig. 3). When contrasting Lower with Upper Holocene, 62 of these peaks gain significance while 24 loose it. We also checked for prominent frequencies: neither the presence of modes nor their changes did accumulate in particular spectral windows. Instead, we found a relatively flat histogram of significant frequency bands (Fig. 3).

3.2 Regional clustering of spectral properties

Only a minority of sites reveal significant modes in the Lower Holocene. After applying the clustering algorithm, absence of oscillations is globally the norm except for small regions in the North Atlantic (tropical western and northern parts), East Africa and Antarctica (red areas in Fig. 4). In the Upper Holocene, North Atlantic and in

particular eastern American sites with dominant modes build large regional clusters. The global distribution of locations with changes in spectral modes displayed in Fig. 5 demonstrates that these are remarkably homogeneous within these regional clusters. Clusters are generally made out of about 4–9 sites with independent proxy records which, in their large majority, exhibit the same spectral trend.

Obviously, damping or amplification of a climate fluctuation mode is only modestly affected by the heterogeneous quality of records, inherent random noise or other local phenomena. The spectral differences between the two selected temperature related records shown above, i.e. for Southeast Europe and Bolivia, can therefore be extrapolated to collections of large areas at sub-continental scale. Like for the two centennial cycles at Sajama, new modes appear during the Mid-Holocene in North and entire South-West America, East and North Atlantic and East Asia. Contrary, climate fluctuations fade out in eastern South America/West Atlantic, the Arctic, East Africa and, to some extent also South-East Asia.

The spatial organization of clusters persist after mapping the change for two frequency sub-domains. In Fig. 6, Mid-Holocene trends separated according centennial and millennial cycles still occur in great spatial uniformity. Since the total band-width is higher for all centennial modes, their global trend pattern also largely resemble the one for the entire frequency band (1/200 yr–1/1800 yr), with the exception that the disappearance of regular climate shifts in the East Atlantic is less pronounced. The clustering in Fig. 5 as well as the differentiated spectral map (Fig. 6) reveal a clear longitudinal pattern. For example, nearly all East Pacific sites become more oscillatory while the contrary happened for the entire Southwest Atlantic. Overall, cycles with periods smaller than 850 yr are more likely to be enhanced in the Upper Holocene compared to millenial modes.

3.3 Cross-validation with trends in non-cyclic event frequency

Our second indicator for the spatio-temporal organization of climate variability which is the density change in non-cyclic events from the first to the second half of the Holocene,

turns out to be spatially coherent as well (Fig. 7). Though, the longitudinal separation for non-cyclic frequency change is differently oriented compared to the Lomb-Scargle derived trends in Fig. 5. Abundance of climatic shifts is, for example, decreasing in East Asia where due to the spectral picture one would expect an increase. However, the pronounced Mid-Holocene enhancement of climate variability in a Pan-American corridor is equally reproduced, and the increase in periodic spectral power in the East Atlantic corridor is corroborated for the southern part. The analysis of non-cyclic events also confirms spatial patterns in centennial spectral trends (Fig. 6, left).

4 Spectral divorce at Mid-Holocene

From the literature on Holocene climate variability one could expect that at least four frequencies play a privileged role in our spectral analysis. The two millennial scale oscillations which comprise the 900 yr periodicity extracted in the GISP2 δ^{18}O records by Schulz and Paul (2002); Rimbu et al. (2004) and the classical 1450 yr period (e.g. O'Brien et al., 1995) are points of reference for many paleo-proxy studies. In addition, a 320 yr and a 550 yr cycle have been repeatedly observed in proxy records as well as output of general circulation models (GCM) with reduced complexity (Weijer and Dijkstra, 2003; Weber et al., 2004; Te Raa and Dijkstra, 2003). However, none of the four modes arose more prominently than others within our global study. The most robust result, instead, derives from an apparent non-stationary of regular climate oscillations. Only about 10% of spectral peaks are stable, i.e. found over the entire period as well as after partial boostrapping. This substantiates our hypothesis that around the 5.5 kyr event (termination of the African Humid Period) the climate system may have undergone an irreversible re-organization. So far, non-stationary variability has only been reported for regional systems, like the Southern Pacific with its decadal to centennial cyclicity related to the El Niño Southern Oscillation (ENSO, Moy et al., 2002). Previous review studies, however, weren't aware of the global dimension of the re-organization between Lower and Upper Holocene. One reason for this may be the

reference character of Greenland and the North Atlantic. Records from this area show persistent millennial cycles (Bond et al., 1997c), in contrast to nearly all other locations around the globe. There, a temporal switch of modes is more often found than their persistence.

A second major outcome of our study is the regional uniformity of temporal trends. Although coverage of many regions is yet much below a value that allows for statistically firm conclusions, the similar, albeit not equal, global distribution of changes in periodic (Fig. 5 as well as non-periodic (Fig. 7) modes and the consistent clustering of adjacent sites which, in general, comprise different proxy types, should be taken as a strong indication for a regionalization of variability modes. Equal trends are even more homogeneously clustered for non-periodic climate variability. They remarkably differ from cyclic trends in Eurasia. Nevertheless, all modes (centennial, millennial and non-cyclic) intensified during the Holocene in a longitudinal zone crossing the Peruvian upwelling area and North-east America. A counterexample, though, against spatial uniformity is evident through the scatter of modal trends within the East Asian monsoon system. This may be due to its internal complexity and various active teleconnections to which the monsoon is sensitive. For example, it has been speculated that the atmospheric connection between the western Asian monsoon and the thermohaline circulation (THC) in the North Atlantic decreased in intensity from the Lower to the Upper Holocene (Morrill et al., 2003). This might explain a reduced correlation between trends in millenial and non-cyclic modes in the two climate sub-systems observed in our study.

5 Possible mechanisms for variability changes

In face of the fragmented understanding of the mechanisms producing climate shifts or quasi-cyclic fluctuations during the Holocene, it seems premature to ask for what may have caused their temporal change or their regional organization. We here only briefly discuss the possible role of ocean and atmospheric circulation, and of external

forcings.

The sun's influence on Holocene climate variability has been deduced from the synchronicity of climate anomalies and variations in solar activity (e.g. Bond et al., 2001c; Hodell et al., 2001c). Our analysis includes records of cosmogenic nuclide production (^{10}Be and ^{14}C flux) as well as reconstructed sunspot number of **?**, and shows persistence of the 208 yr Suess cycle together with a damping of millennial modes after 6 kyr BP (Fig. 2 and yellow sun in Figs. 5–6). A recent analysis of the sunspot number power spectrum (Dima and Lohmann, 2005) identified periods of 6,500, 2,500, 950 and 550 yr. Debret et al. (2007) already questioned the hypothesis of Bond et al. (2001a) that the 1500 yr cycles are due to variations in solar activity. Still, the possibility of solar variability being amplified by oceanic feedbacks can not be entirely excluded (Renssen et al., 2006).

Central in the literature discussion is the THC, which is connected to North Atlantic deep water formation. The THC is commonly considered the primary process for the generation of climate fluctuations on interdecadal or centennial (Broecker et al., 1985) as well as millennial time scales (Stocker et al., 1992; Weijer and Dijkstra, 2003). Schulz and Paul (2002), however, questioned its connection with the prominent 1450 yr oscillation. The Iceland–Scotland overflow water is an important component of the thermohaline circulation. Its record contains dominant periodicities of 1,400 and 700 years associated with THC variations over the Holocene (Bianchi and McCave, 1999). It is conceivable that ocean circulation changes, like those of the Atlantic multidecadal oscillations, modulate SST variability in the North Atlantic basin on centennial and longer timescales. Particular THC variations are detected for the Mid-Holocene in the ocean circulation through hydrographic changes (Rühlemann et al., 2004), which were more pronounced in the early Holocene (Kim et al., 2007).

To understand the atmospheric circulations related to Holocene variability, one can look for analogous patterns during the instrumental period. This procedure was used to explore the physical processes producing SST patterns and thereby to understand recorded Holocene SST changes (Marchal et al., 2002; Rimbu et al., 2004; Lorenz

et al., 2006). The spatial pattern of Northern Hemisphere SST reconstructions for the Holocene emphasizes a North Atlantic Oscillation trend towards its negative phase, a feature which can be reproduced by a coupled climate model (Lorenz and Lohmann, 2004). This trend is overlaid by 2,400 and 900 yr cycles (Rimbu et al., 2004), consistent with other proxy data sets and solar variation.

Other mechanisms behind temporally changing modes include (1) high frequency "noise" (2) low frequency orbital forcing, and (3) particular events. The Pacific decadal oscillation and the El Niño-Southern Oscillation (ENSO) show long-term enhancement (Moy et al., 2002; Rimbu et al., 2004). The origin of high frequency fluctuations is controversially discussed but a combination of nonlinear oceanographic interactions in the tropical Pacific and orbital forcing well fits into model-based and instrumental evidence (Clement et al., 1999; Loubere et al., 2003). These fluctuations may have activated multicentennial modes (Simmonds and Walland, 1998). Phase transitions in climate sub-systems could also be triggered by a slow change in insolation. Given the wider distribution of millennial modes after the cessation of oscillations in solar activity at 6 kyr BP, we suggest that the Mid-Holocene reversal of insolation change differently affected regional subsystems. As a result, oceanic or atmospheric teleconnections between subsystems could have weakened or strengthened. Such shifts were possibly mediated by dislocations of convergence zones or trade winds, thereby modifying the damping and amplification forces of modes (Lohmann and Lorenz, 2007).

Intensification of ENSO in the Mid-Holocene, with a progressive increase in frequency to periodicities of 2 to 8.5 years, is believed to mark the onset of modern-day precipitation patterns in low-latitude regions (Rodbell et al., 1999). Analysis of archives in northern Africa indicate strong reductions in tropical trees and Sahelian grassland cover, which allowed large-scale dust mobilization after 4300 yr BP (Kropelin et al., 2008). Haug et al. (2001) found a large transition (in the frequency space) at Cariaco Basin ∼3800 years ago indicative for tropical reorganization of the hydrological cycle. Similar millennial-scale hydrologic variability is reported at other locations (Koutavas et al., 2002; Ekdahl et al., 2005).

Most of the transitions overstress the capabilities of concurrent climate models, but it is useful to compare the induced variability with internal oscillatory modes (without external trigger) which are seen in models of reduced complexity (Mikolajewicz and Maier-Reimer, 1990; Weijer and Dijkstra, 2003). Model perturbation experiments reveal eigenmodes on millennial time scales. These modes are generated by the advection of buoyancy anomalies around the overturning loop, both in a single-hemispheric basin leading to centennial modes or throughout the global ocean responsible for millennial cycles. The most negative eigenvalues (strongest damping) was found for centennial oscillations (Weijer and Dijkstra, 2003; Te Raa and Dijkstra, 2003). However, such modes could be activated if fluctuations in radiative energy input are included into simulation studies (Weber et al., 2004).

6 Consequences for cultural development?

The evidence that climate variability was not uniformly distributed over the globe, gains a new aspect to the dispute of whether or how Holocene climate affected the development of human societies. We propose that frequency of climate changes rather than average characteristics made an effective difference between inhabited world regions. In particular cultures situated in the Pan-American corridor have seen a significant rise in event frequency by about two additional disruptions more per millenium after 6 kyr BP. It is well imaginable that increased climate variability meant an elevated stress for early American societies. Repeated cultural discontinuities go well beyond the effects of singular events. In western Asia, like in many other world regions, the probability of climatic shifts (also visible as centennial modes) declined over the Holocene. Ancient civilizations in the Near East or later in southern Europe were challenged by abrupt climatic changes and resulting subsistence crises with much lower frequency. In his Pullitzer price winning work, J. Diamond related the lagged development between Old and New World before the colonization era to differences in biodiversity determined by the geographical orientation of the Americas with respect to Eurasia (Diamond,

1999). We here suggest that climate variability should be taken into consideration in these conceptual approaches and also in quantitative approaches to simulating the effect of climate on human prehistory (e.g., Wirtz and Lemmen, 2003).

7 Conclusions

Our analysis substantiates two hypotheses. First, the propensity of the climate system to amplify external fluctuations or to endogenously generate them is not a global property, but differs among regions. Secondly, most regional propensities underwent a irreversible change during the Mid-Holocene. Fluctuations especially intensified along a Pan-American corridor. This eventually led to an unequal probability of crisis for early human civilizations in the Old and New World.

Our study did not produce evidence for millennial scale cyclicity in solar activity proxies for the Upper Holocene, nor for a privileged role of the prominent 250, 550, 900 and 1450 yr cycles. This finding corroborates the regional nature of climate variability. It seems likely that altered ocean circulation together with slightly modified coupling intensity between subsystems (regional interplay of ice, ocean, atmosphere and vegetation) after the 5.5 kyr BP event made these subsystems either more or less prone to oscillations. The discussion of possible mechanisms behind changed climate variability, however, has to be substantiated by future modelling studies.

Acknowledgements. We thank Karin Holmgren, Detlef Gronenborn, Hans von Storch, Dennis Bray, Victor Brovkin for helpful comments on an earlier version of the manuscript. Sabrina Solms and Sonja Dorendorf are acknowledged for assisting with the compilation of data and literature. C. L. was supported by the Deutsche Forschungsgemeinschaft (DFG priority program INTERDYNAMIK) and the Dutch Agency for Environmental Assessment (MNP Bilthoven).

References

Abbott, M., Binford, M. W., Brenner, M., Curtis, J. H., and Kelts, K. R.: A 3,500 ^{14}C yr high-resolution sediment record of lake level changes in Lake Titicaca, Bolivia/Peru, Quatern. Res., 47, 169–180, 1997. 318

Anderson, D. G.: Climate and culture change in Prehistoric and Early Historic North America, Archaeol. Eastern N. Am., 29, 143–186, 2001. 289

Andreev, A., Tarasov, P., Siegert, C., Ebel, T., Klimanov, V., Melles, M., Hahne, J., Shilova, G., Dereviagin, A., and Hubberten, H.-W.: Vegetation and climate changes on the northern Taymyr, Russia during the Upper Pleistocene and Holocene reconstructed from pollen records, Boreas, 32, 484–505, 2003. 319

Arz, H. W., Gerhardt, S., Pätzold, J., and Röhl, U.: Millennial-scale changes of surface- and deep-water flow in the western tropical Atlantic linked to Northern Hemisphere high-latitude climate during the Holocene, Geology, 29, 239–242, 2001. 318

Bahr, A., Lamy, F., Arz, H., Kuhlmann, H., and Wefer, G.: Late glacial to Holocene climate and sedimentation history in the NW Black Sea, Mar. Geol., 214, 309–322, 2005. 318

Bar-Matthews, M., Ayalon, A., Kaufman, A., and Wasserburg, G. J.: The Eastern Mediterranean paleoclimate as a reflection of regional events: Soreq cave, Israel, Earth and Planet. Sci. Lett., 166, 85–95, 1999. 318

Barber, D., Dyke, A., Hillaire-Marcel, C., Jennings, A., Andrews, J., et al.: Forcing of the cold event of 8200 years ago by catastrophic drainage of Laurentide lakes, Nature, 400, 344–348, 1999. 318

Barber, K., Zolitschka, B., Tarasov, P., and Lotter, A. F.: Atlantic to Urals – the Holocene climatic record of Mid-Latitude Europe, in: Past Climate Variability through Europe and Africa, edited by R.W. Battarbee, F. G. and Stickley, C., vol. 6 of *Developments in Paleoenvironmental Research*, Springer, Dordrecht, 2004. 289

Barker, P. A., Street-Perrott, F. A., Leng, M. J., Greenwood, P. B., Swain, D. L., Perrott, R. A., Telford, R. J., and Ficken, K. J.: A 14 000-Year Oxygen Isotope Record from Diatom Silica in Two Alpine Lakes on Mt. Kenya, Science, 292, 2307–2310, 2001. 318, 319

Benson, L., Kashgarian, M., Rye, R., Lund, S., Paillet, F., Smoot, J., Kester, C., Mensing, S., Meko, D., and Lindström, S.: Holocene multidecadal and multicentennial droughts affecting Northern California and Nevada, Quatern. Sci. Rev., 21, 659–682, 2002. 318

Bianchi, G. and McCave, I.: Holocene periodicity in North Atlantic climate and deep-ocean flow

south of Iceland, Nature, 397, 515–517, 1999. 298
Binford, L. R.: Constructing Frames of Reference, University of California Press, Berkeley and Los Angeles, 2001. 289
Bond, G., Showers, W., Cheseby, M., Lotti, R., Almasi, P., deMenocal, P., Priore, P., Cullen, H., Hajdas, I., and Bonani, G.: A pervasive millennial-scale cycle in North Atlantic Holocene and glacial climates, 1257–1266, 1997a. 318
Bond, G., Showers, W., Cheseby, M., Lotti, R., Almasi, P., deMenocal, P., Priore, P., Cullen, H., Hajdas, I., and Bonani, G.: A pervasive millennial-scale cycle in North Atlantic Holocene and glacial climates, Science, 278, 1257–1266, 1997b.
Bond, G., Showers, W., Cheseby, M., Lotti, R., Almasi, P., deMenocal, P., Priore, P., Cullen, H., Hajdas, I., and Bonani, G.: A pervasive millennial-scale cycle in North Atlantic Holocene and glacial climates, 1257–1266, 1997c. 288, 290, 297
Bond, G., Kromer, B., Beer, J., Muscheler, R., Evans, M. N., Showers, W., Hoffmann, S., Lotti-Bond, R., Hajdas, I., and Bonani, G.: Persistent Solar Influence on North Atlantic Climate During the Holocene, 2130–2136, 2001a. 298, 318
Bond, G., Kromer, B., Beer, J., Muscheler, R., Evans, M. N., Showers, W., Hoffmann, S., Lotti-Bond, R., Hajdas, I., and Bonani, G.: Persistent Solar Influence on North Atlantic Climate During the Holocene, Science, 294, 2130–2136, 2001b.
Bond, G., Kromer, B., Beer, J., Muscheler, R., Evans, M. N., Showers, W., Hoffmann, S., Lotti-Bond, R., Hajdas, I., and Bonani, G.: Persistent Solar Influence on North Atlantic Climate During the Holocene, 2130–2136, 2001c. 290, 291, 298, 316
Bonnefille, R. and Chalie, F.: Pollen-inferred precipitation time-series from equatorial mountains, Africa, the last 40 kyr BP, Global Planet. Change, 26, 25–50, 2000. 318
Brachfeld, S., Acton, G. D., Guyodo, Y., and Banerjee, S. K.: High-resolution paleomagnetic records from Holocene sediments from the Palmer Deep, Western Antartic Peninsula, Earth and Planet. Sci. Lett., 181, 429–441, 2000. 318
Broecker, W., Peteet, D., and Rind, D.: Does the ocean-atmosphere system have more than one stable mode of operation?, Nature, 315, 21–25, 1985. 298
Camill, P., Umbanhowar, C. E., Teed, R., Geiss, C. E., Aldinger, J., et al.: Late-glacial and Holocene climatic effects on fire and vegetation dynamics at the prairie forest ecotone in south-central Minnesota, J. Ecol., 91, 822–836, 2003. 318
Carcaillet, C., Bergeron, Y., Richard, P., Fréchette, B., Gauthier, S., and Prairie, Y.: Change of fire frequency in the eastern Canadian boreal forests during the Holocene: does vegetation

composition or climate trigger the fire regime?, J. Ecol., 89, 930–946, 2001. 318
Chapman, M. R. and Shackleton, N. J.: Evidence of 550-year and 1000-year cyclicities in North Atlantic circulation patterns during the Holocene, Holocene, 10, 287–291, 2000. 318
Claussen, M., Kubatzki, C., Brovkin, V., Ganopolski, A., Hoelzmann, P., and Pachur, H.: Simulation of an abrupt change in Saharan vegetation at the end of the mid-Holocene, Geophys. Res. Lett., 24, 2037–2040, 1999. 289
Clement, A., Seager, R., and Cane, M.: Orbital controls on the El Niño Southern Oscillation and the tropical climate, Paleoceanography, 14, 441–456, 1999. 299
Cook, E., Buckley, B., D'Arrigo, R., and Peterson, M.: Warm-season temperatures since 1600 BC reconstructed from Tasmanian tree rings and their relationship to large-scale sea surface temperature anomalies, Clim. Dynam., 16, 79–91, 2000. 319
Coombes, P. and Barber, K.: Environmental determinism in Holocene research: causality or coincidence?, Area, 37, 303–311, 2005. 289
Cruz, F., Burns, S., Karmann, I., Sharp, W., Vuille, M., Cardoso, A., Ferrari, J., Dias, P. S., and Jr., O. V.: Insolation-driven changes in atmospheric circulation over the past 116 000 years in subtropical Brazil, Nature, 434, 63–66, 2005. 318
Curtis, J., Brenner, M., and Hodell, D.: Climate change in the Lake Valencia Basin, Venezuela, ≈12 600 yr BP to present, Holocene, 9, 609–619, 1999. 318
Curtis, J. H., Brenner, M., Hodell, D. A., Balser, R. A., Islebe, G. A., and Hooghiemstra, H.: A multi-proxy study of Holocene environmental change in Lowlands of Peten, Guatemala, J. Paleolimnol., 19, 139–159, 1998. 318
Davis, B. A. S., Brewer, S., Stevenson, A. C., Guiot, J., and Data Contributors: The temperature of Europe during the Holocene reconstructed from pollen data, Quatern. Sci. Rev., 22, 1597–1629, 2003a. 318
Davis, B. A. S., Brewer, S., Stevenson, A. C., Guiot, J., and Data Contributors: The temperature of Europe during the Holocene reconstructed from pollen data, Quatern. Sci. Rev., 22, 1597–1629, 2003b. 321
Davis, O. K.: Rapid Climate Change in Coastal Southern California Inferred from Pollen analysis of San Joaquin Marsh, Quatern. Res., 23, 227–235, 1992. 318
Debret, M., Bout-Roumazeilles, V., Grousset, F., Desmet, M., McManus, J. F., Massei, N., Sebag, D., Petit, J.-R., Copard, Y., and Trentesaux, A.: The origin of the 1500-year climate cycles in Holocene North-Atlantic records, Clim. Past, 3, 569–575, 2007, http://www.clim-past.net/3/569/2007/. 290, 298

deMenocal, P., Ortiz, J., Guilderson, T., and Sarnthein, M.: Coherent high- and low-latitude climate variability during the Holocene warm period, Science, 288, 2198–2202, 2000a. 318
deMenocal, P., Ortiz, J., Guilderson, T., and Sarnthein, M.: Coherent high- and low-latitude climate variability during the Holocene warm period, Science, 288, 2198–2202, 2000b. 289, 290
deMenocal, P. B.: Cultural responses to climate change during the late Holocene, Science, 292, 667–673, 2001. 289
Denniston, R., Gonzalez, L., Baker, R.G.and Reagan, M., Asmerom, Y., Edwards, R., and Alexander, E.: Speleothem evidence for Holocene fluctuations of the prairie-forest ecotone, north-central USA, Holocene, 9, 671–676(6), 1999. 318
Diamond, J.: Guns, germs, and steel: the fates of human societies, W. W. Norten & Company, 1999. 300
Dima, M. and Lohmann, G.: Conceptual model for millennial climate variability: a possible combined solar-thermohaline circulation origin for the 1500-year cycle, Clim. Dynam., 10, 301–311, 2005. 298
Doose-Rolinski, H., Rogalla, U., Scheeder, G., Lückge, A., and von Rad, U.: High resolution temperature and evaporation changes during the late Holocene in the northeastern Arabian Sea, Palaeooceanography, 16, 358–367, 2001. 319
Dorale, J., Gonzalez, L., Reagan, M., Pickett, D., Murrell, M., and Baker, R.: A high resolution record of Holocene climate change in speleothem calcite from Cold Water Cave, northeast Iowa, Science, 258, 1626–1630, 1992. 318
Drysdale, R., Zanchetta, G., Hellstrom, J., Maas, R., Fallick, A., Pickett, M., Cartwright, I., and Piccini, L.: Late Holocene drought responsible for the collapse of Old World civilizations is recorded in an Italian cave flowstone, Geology, 34, 101–104, 2006. 318
Ekdahl, E. J., Fritz, S. C., Baker, P. A., Rigsby, C. A., and Coley, K.: Holocene multidecadal- to millennial-scale hydrologic variability on the South American Altiplano, The Holocene, 18, 867–876, 2005. 299
Erickson, C. L.: Neo-environmental determinism and agrarian “collapse” in Andean prehistory, Antiquity, 73, 634–642, 1999. 289
Fagan, B.: Floods, Famines, And Emperors: El Nino And The Fate Of Civilizations, Basic Books, University of California, Santa Barbara, 1999. 289
Fairbridge, R. and Hillaire-Marcel, C.: An 8,000-yr palaeoclimatic record of the ”Double-Hale” 45-yr solar cycle, Nature, 268, 413–416, 1977. 288, 290

Fengming, C., Tiegang, L., Lihua, Z., and Jun, Y.: A Holocene paleotemperature record based on radiolaria from the northern Okinawa Trough (East China Sea), Quat. Int., 183, 115–122, 2008. 319
Finkel, R. and Nishiizumi, K.: Beryllium 10 concentrations in the Greenland Ice Sheet Project 2 ice core from 3-40 ka, J. Geophys. Res., 102, 26 699–26 706, 1997. 318
Fleitmann, D., Burns, S. J., Mudelsee, M., Neff, U., Kramers, J., Mangini, A., and Matter, A.: Holocene Forcing of the Indian Monsoon Recorded in a Stalagmite from Southern Oman, Science, 300, 1737–1739, 2003. 319
Fleitmann, D., Burns, S., Mangini, A., Mudelsee, M., Kramers, J., Villa, I., Neff, U., Al-Subbary, A., Buettner, A., Hippler, D., et al.: Holocene ITCZ and Indian monsoon dynamics recorded in stalagmites from Oman and Yemen (Socotra), Quaternary Science Reviews, 26, 170–188, 2007. 319
Fontes, J.-C., Gasse, F., and Gibert, E.: Holocene environmental changes in Lake Bangong basin (Western Tibet). Part 1: Chronology and stable isotopes of carbonates of a Holocene lacustrine core, Paleogeogr. Palaeoclimatol. Palaeoecol., 120, 25–47, 1996. 319
Freudenthal, T., Meggers, H., Henderiks, J., Kuhlmann, H., Moreno, A., and Wefer, G.: Upwelling intensity and filament activity off Morocco during the last 250,000 years, Deep-Sea Res. II, 49, 3655–3674, 2002. 318
Gasse, F.: Hydrological changes in the African tropics since the Last Glacial Maximium, Quat. Sci. Revi., 19, 189–211, 2000. 319
Gasse, F.: Diatom-inferred salinity and carbonate oxygen isotopes in Holocene waterbodies of the western Sahara and Sahel (Africa), Quatern. Sci. Rev., 21, 737–767, 2002. 318
Grootes, P. and Stuiver, M.: Oxygen 18/16 variability in Greenland snow and ice with 10^{-3}- to 10^{5}-year time resolution, J. Geophys. Res., 102, 26 455–26 470, 1997. 318
Grootes, P. M., Steig, E. J., Stuiver, M., Waddington, E. D., and Morse, D. L.: A new ice core record from Taylor Dome, Antarctica, Eos, 75, p. 225, 1994. 319
Gupta, A., Anderson, D., and Overpeck, J.: Abrupt changes in the Asian southwest monsoon during the Holocene and their links to the North Atlantic Ocean, Nature, 421, 354–356, 2003. 318, 319
Hantemirov, R. M. and Shiyatov, S. G.: A continuous multi-millennial ring-width chronology in Yamal, northwestern Siberia, Holocene, 12, 717–726, 2002. 319
Haug, G. H., Hughen, K. A., Sigman, D. M., Peterson, L. C., and Röhl, U.: Southward migration of the intertropical convergence zone through the Holocene, Science, 293, 1304, 2001. 299,

318
Herzschuh, U., Tarasov, P., Wünnemann, B., and Hartmann, K.: Holocene vegetation and climate of the Alashan Plateau, NW China, reconstructed from pollen data, Paleogeogr. Palaeoclimatol. Palaeoecol., 211, 1–17, 2004. 319
Higuera-Gundy, A., Brenner, M., Hodell, D. A., Curtis, J. H., Leyden, B. W., and Binford, M. W.: A 10 300 ^{14}C yr record of climate and vegetation change from Haiti, Quat. Res., 52, 159–170, 1999. 318
Hodell, D., Curtis, J. H., and Brenner, M.: Possible role of climate in the collapse of the Classic Maya Civilization, Nature, 375, 391–394, 1995. 318
Hodell, D., Curtis, J., Sierro, F., and Raymo, M.: Correlation of late Miocene to early Pliocene sequences between the Mediterranean and North Atlantic, Paleoceanography, 16, 164–178, 2001a. 318
Hodell, D., Kanfoush, S., Shemesh, A., Crosta, X., Charles, C., and Guilderson, T.: Abrupt Cooling of Antarctic Surface Waters and Sea Ice Expansion in the South Atlantic Sector of the Southern Ocean at 5000 cal yr B.P., Quatern. Res., 56, 191–198, 2001b. 318
Hodell, D. A., Brenner, M., Curtis, J. H., and Guilderson, T.: Solar Forcing of Drought Frequency in the Maya Lowlands, Science, 292, 1367–1370, 2001c. 290, 298
Holmgren, K., Lee-Thorp, J., Cooper, G., Lundblad, K., Partridge, T., Scott, L., Sithaldeen, R., Talma, A., and Tyson, P.: Persistent Millennial-Scale Climatic Variability Over the Past 25 thousand Years in Southern Africa, Quatern. Sci. Rev., 22, 2311–2326, 2003. 318
Hu, F. S., Ito, E., Brubaker, L. B., and Anderson, P. M.: Ostracode Geochemical Record of Holocene Climatic Change and Implications for Vegetational Response in the Northwestern Alaska Range, Quatern. Res., 49, 86–95, 1998. 318
Huang, C.-Y., Liew, P.-M., Zhao, M., Chang, T.-C., Kuo, C.-M., Chen, M.-T., Wang, C.-H., and Zheng, L.-F.: Deep sea and lake records of the Southeast Asian paleomonsoons for the last 25 thousand years, Earth and Planet. Sci. Lett., 146, 59–72, 1997. 319
Hughes, M. K. and Graumlich, L. J.: Climatic variations and forcing mechanisms of the last 2000 years. Multi-millenial dendroclimatic studies from the western United States, NATO ASI Series, 141, 109–124, 1996. 318
Husum, K. and Hald, M.: A continuous marine record 8000–1600 cal. yr BP from the Malangenfjord, north Norway: foraminiferal and isotopic evidence, The Holocene, 14, 877–887, 2004. 318
Jin, Z., Wu, J., Cao, J., Wang, S., Shen, J., Gao, N., and Zou, C.: Holocene chemical weathering

and climatic oscillations in north China: evidence from lacustrine sediments, Boreas, 33, 260–266, 2004. 319
Johnson, T. C., Brown, E. T., McManus, J., Barry, S., Barker, P., and Gasse, F.: A High-Resolution Paleoclimate Record Spanning the Past 25, 000 Years in Southern East Africa, Science, 296, 113–132, 2002. 318
Jones, V. J., Leng, M. J., Solovieva, N., Sloaneb, H. J., and Tarasovc, P.: Holocene climate of the Kola Peninsula; evidence from the oxygen isotope record of diatom silica, Quatern. Sci. Rev., 23, 833–839, 2004. 318
Jung, S., Davies, G., Ganssen, G., and Kroon, D.: Synchronous Holocene sea surface temperature and rainfall variations in the Asian monsoon system, Quatern. Sci. Rev., 23, 2207–2218, 2004. 319
Keigwin, L. D.: The little Ice Age and medieval warm period in the Sargasso Sea, Science, 274, 1503–1508, 1996. 318
Kienast, M., Calvert, S. E., Pelejero, C., and Grimalt, J. O.: A critical review of marine sedimentary δ^{13}Corg-pCO_2 estimates: New palaeorecords from the South China Sea and a revisit of other low-latitude δ^{13}C org-pCO_2 records, Global Biogeochem. Cy., 15, 113–127, 2001. 319
Kim, J., Meggers, H., Rimbu, N., Lohmann, G., Freudenthal, T., Muller, P., and Schneider, R.: Impacts of the North Atlantic gyre circulation on Holocene climate off northwest Africa, Geology, 35, 387–390, 2007. 289, 298
Kim, J.-H. and Schneider, R. R.: Low-latitude control of interhemispheric sea-surface temperature contrast in the tropical Atlantic over the past 21 kyears: the possible role of SE trade winds, Clim. Dynam., 21, 337–347, 2003. 318
Knaack, J.: Eine neue Transferfunktion zur Rekonstruktion der Paläoproduktivität aus Gemeinschaften mariner Diatomeen, Berichte Rep. Geol. Paläontologisches Inst. Univ.t Kiel, 83, 1–118, 1997. 318
Koutavas, A., Lynch-Stieglitz, J., Marchitto, T., and Sachs, J.: El Niño-Like Pattern in Ice Age Tropical Pacific Sea Surface Temperature, Science, 297, 226–230, 2002. 299
Kropelin, S., Verschuren, D., Lezine, A., Eggermont, H., Cocquyt, C., Francus, P., Cazet, J., Fagot, M., Rumes, B., Russell, J., et al.: Climate-Driven Ecosystem Succession in the Sahara: The Past 6000 Years, Science, 320, 765–768, 2008. 299
Lachniet, M., Asmerom, Y., Burns, S., Patterson, W., Polyak, V., and Seltzer, G.: Tropical response to the 8200 yr B.P. cold event? Speleothem isotopes indicate a weakened early Holocene monsoon in Costa Rica, Geology, 32, 957–960, 2004. 318

Laird, K. R., Fritz, S. C., Maasch, K. A., and Cumming, B. F.: Greater drought intensity and frequency before A.D. 1200 in the northern Great Plains, USA, Nature, 384, 552–554, 1996. 318

Lamy, F., Hebbeln, D., Röhl, U., and Wefer, G.: Holocene rainfall variability in southern Chile: a marine record of latitudinal shifts of the Southern Westerlies, Earth and Planet. Sci. Lett., 185, 369–382, 2001. 318

Lamy, F., Rühlemann, C., Hebbeln, D., and Wefer, G.: High- and low-latitude climate control on the position of the southern Peru-Chile Current during the Holocene, Palaeooceanography, 17, 1028, doi:10.1029/2001PA000727, 2002. 318

Lea, D., Pak, D., Peterson, L., and Hughen, K.: Synchroneity of tropical and High-Latitude Atlantic Temperatures over the last glacial termination, Science, 301, 1361–1364, 2003. 318

Liu, J., Houyuan, L., Negendank, J., Mingram, J., Xiangjun, L., Wenyuan, W., and Guoqiang, C.: Periodicity of Holocene climatic variations in the Huguangyan Maar Lake, Chinese Sci. Bull., 45, 1712–1718, 2000a. 319

Liu, Z., Kutzbach, J., and Wu, L.: Modeling climate shift of El Nino variability in the Holocene., Geophys. Res. Lett., 27, 2265–2268, 2000b.

Lohmann, G. and Lorenz, S. J.: Orbital forcing on atmospheric dynamics during the last interglacial and glacial inception, in: The climate of past interglacials, edited by Sirocko, F., Claussen, M., Sanchez-Goni, M. F., and Litt, T., vol. 7 of *Developments in Paleoenvironmental Research*, Elsevier, 2007. 299

Lorenz, S. and Lohmann, G.: Acceleration technique for Milankovitch type forcing in a coupled atmosphere-ocean circulation model: method and application for the Holocene, Climate Dynam., 23, 727–743, 2004. 299

Lorenz, S., Kim, J., Rimbu, N., Schneider, R., and Lohmann, G.: Orbitally driven insolation forcing on Holocene climate trends: Evidence from alkenone data and climate modeling, Palaeooceanography, 21, PA1002, doi:10.1029/2005PA001152, 2006. 298

Loubere, P., Richaud, M., Liu, Z., and Mekik, F.: Oceanic conditions in the eastern equatorial Pacific during the onset of ENSO in the Holocene, Quat. Res., 60, 142–148, 2003. 299

Marchal, O., Cacho, I., Stocker, T., Grimalt, J., Calvo, E., Martrat, B., Shackleton, N., Vautravers, M., Cortijo, E., van Kreveld, S., et al.: Apparent long-term cooling of the sea surface in the northeast Atlantic and Mediterranean during the Holocene, Quatern. Sci. Rev., 21, 455–483, 2002. 298

Masson, V., Vimeux, F., Jouzel, J., Morgan, V., Delmotte, M., et al.: Holocene climate variability

in Antarctica based on 11 ice-core isotopic records, Quatern. Res., 54, 348–358, 2000. 319

Mayewski, P., Rohling, E., Stager, J., Karlen, W., Maasch, K., Meeker, L., Meyerson, E., Gasse, F., Kreveld, S., Holmgren, K., et al.: Holocene climate variability, Quatern. Res., 62, 243–255, 2004. 288, 289, 290, 291

McDermott, F.: Palaeo-climate reconstruction from stable isotope variations in speleothems: a review, Quatern. Sci. Rev., 23, 901–918, 2004. 318

McDermott, F., Mattey, D., and Hawkesworth, C.: Centennial-scale Holocene climate variability revealed by a high-resolution speleothem δ^{18}O record from S.W. Ireland, Science, 294, 1328–1331, 2001. 290

Mikolajewicz, U. and Maier-Reimer, E.: Internal secular variability in an ocean general circulation model, Clim. Dynam., 4, 145–156, 1990. 300

Moberg, A., Sonechkin, D., Holmgren, K., Datsenko, N., and Karlin, W.: Highly variable Northern Hemisphere temperatures reconstructed from low- and high-resolution proxy data, Nature, 433, 613–617, 2005. 289, 290, 292

Morrill, C., Overpeck, J., and Cole, J.: A synthesis of abrupt changes in the Asian summer monsoon since the last deglaciation, The Holocene, 13, 465–476, 2003. 290, 292, 297

Moy, C., Seltzer, G. O., Rodbell, D. T., and Anderson, D. M.: Variability of El Niño/Southern Oscillation activity at millennial timescales during the Holocene epoch, Nature, 420, 162–165, 2002. 292, 296, 299, 318

Noren, A., Bierman, P., Steig, E., Lini, A., and Southon, J.: Millennial-scale Storminess Variability in the Northeastern United States during the Holocene Epoch, 821–824, 2002a. 318

Noren, A., Bierman, P., Steig, E., Lini, A., and Southon, J.: Millennial-scale Storminess Variability in the Northeastern United States during the Holocene Epoch, Nature, 419, 821–824, 2002b. 290, 316

Oba, T. and Murayama, M.: Sea-surface temperature and salinity changes in the northwest Pacific since the Last Glacial Maximum, J. Quat. Sci., 19, 335–346, 2004. 318

O'Brien, S. R., Mayewski, P. A., Meeker, L. D., Meese, D. A., Twickler, M. S., and Whitlow, S. I.: Complexity of Holocene Climate as Reconstructed from a Greenland Ice Core, Science, 270, 1962–1964, 1995. 296

Petit, J. R., Jouzel, J., Raynaud, D., Barkov, N. I., Barnola, J.-M., et al.: Climate and atmospheric history of the past 420, 000 years from the Vostok ice core, Antarctica, Nature, 399, 429–436, 1999. 319

Renssen, H., Goosse, H., Fichefet, T., and Campin, J.: The 8.2 kyr BP event simulated by a

global atmosphere sea-ice ocean model., Geophys. Res. Lett., 28, 1567–1570, 2001. 289
Renssen, H., Goosse, H., and Muscheler, R.: Coupled climate model simulation of Holocene cooling events: oceanic feedback amplifies solar forcing, Clim. Past, 2, 79–90, 2006, http://www.clim-past.net/2/79/2006/. 298
Richerson, P. J., Boyd, R., and Bettinger, R. L.: Was agriculture impossible during the Pleistocene but mandatory during the Holocene? A Climate Change Hypothesis, Archaeol. Austriaca, 66, 1–50, 2001. 288
Ricketts, R. D., Johnson, T. C., Brown, E. T., Rasmussen, K. A., and Romanovsky, V. V.: The Holocene paleolimnology of Lake Issyk-Kul, Kyrgyzstan: trace element and stable isotope composition of ostracodes, Palaeogeogr., Palaeoclimatol., Palaeoecol., 176, 207–227, 2001. 316, 319
Rimbu, N., Lohmann, G., Lorenz, S., Kim, J., and Schneider, R.: Holocene climate variability as derived from alkenone sea surface temperature and coupled ocean-atmosphere model experiments, Climate Dynam., 23, 215–227, 2004. 289, 296, 298, 299
Rodbell, D., Seltzer, G. O., Anderson, D., Abbott, M., Enfield, D., and Newman, J.: An 15 000-Year Record of El-Niño Alluviation in Southwestern Ecuador, Science, 283, 516–520, 1999. 299, 318
Rosenthal, Y., Oppo, D. W., and Linsley, B. K.: The amplitude and phasing of climate change during the last deglaciation in the Sulu Sea, western equatorial Pacific, Geophys. Res. Lett., 30, 1428, doi:10.1029/2002GL016612, 2003. 318, 319
Rubensdotter, L. and Rosqvist, G.: The effect of geomorphological setting on Holocene lake sediment variability, northern Swedish Lapland, J. Quat. Sci., 18, 757–767, 2003. 318
Rühlemann, C., Mulitza, S., Lohmann, G., Paul, A., Prange, M., and Wefer, G.: Intermediate depth warming in the tropical Atlantic related to weakened thermohaline circulation: Combining paleoclimate data and modeling results for the last deglaciation, Palaeooceanography, 19, 1025–1035, doi:10.1029/2003PA000948, 2004. 298
Sarkar, A., Ramesh, R., Somayajulu, B., Agnihotri, R., Jull, A., and Burr, G.: High resolution Holocene monsoon record from the eastern Arabian Sea, Earth and Planet. Sci. Lett., 177, 209–218, 2000. 319
Sarnthein, M., van Kreveld, S., Erlenkeuser, H., Grootes, P., Kucera, M., Pflaumann, U., and Schulz, M.: Centennial-to-millennial-scale periodicities of Holocene climate and sediment injections off the western Barents shelf, 75N, Boreas, 32, 447–461, 2003a. 318
Sarnthein, M., van Kreveld, S., Erlenkeuser, H., Grootes, P., Kucera, M., Pflaumann, U., and

Schulz, M.: Centennial-to-millennial-scale periodicities of Holocene climate and sediment injections off the western Barents shelf, 75N, Boreas, 32, 447–461, 2003b. 290
Schilman, B., Almogi-Labin, A., and Bar-Matthews, M.: Late Holocene productivity and hydrographic variability in the eastern Mediterranean inferred from benthic foraminiferal stable isotopes, Palaeooceanography, 18, 1064–1076, 2003. 318
Schulz, H.: Meeresoberflächentemperaturen vor 10:000 Jahren – Auswirkungen des frühholozänen Insolationsmaximums, Berichte-reports, Geologisch-Paläontologischen Institut und Museum, Christian-Albrechts-Universität, Kiel, 1995. 319
Schulz, M. and Mudelsee, M.: REDFIT: Estimating red-noise spectra directly from unevenly spaced paleoclimatic time series, Computers & Geosciences, 28, 421–426, 2002. 292
Schulz, M. and Paul, A.: Holocene Climate Variability on Centennial-to-Millennial Time Scales: 1. Climate Records from the North-Atlantic Realm, in: Climate Development and History of the North Atlantic Realm, edited by: Wefer, G., Berger, W., Behre, K., and Jansen, E., 41–54, Springer, Berlin, 2002. 296, 298
Seeberg-Elverfeldt, I. A., Lange, C. B., Arz, H. W., Pätzold, J., and Pike, J.: The significance of diatoms in the formation of laminated sediments of the Shaban Deep, Northern Red Sea, Mar. Geol., 209, 279–301, 2004. 318
Seppä, H., Birks, H. J. B., Giesecke, T., Hammarlund, D., Alenius, T., Antonsson, K., Bjune, A. E., Heikkilä, M., MacDonald, G. M., Ojala, A. E. K., Telford, R. J., and Veski, S.: Spatial structure of the 8200 cal yr BP event in northern Europe, Clim. Past, 3, 225–236, 2007, http://www.clim-past.net/3/225/2007/. 290
Shimada, C., Ikehara, K., Tanimura, Y., and Hasegawa, S.: Millennial-scale variability of Holocene hydrography in the southwestern Okhotsk Sea: diatom evidence, Holocene, 14, 641–650, 2004. 319
Simmonds, I. and Walland, D. J.: Decadal and centennial variability of the southern semiannual oscillation simulated in the GFDL coupled GCM, Clim. Dynam., 14, 45–53, 1998. 299
Sirocko, F.: What Drove Past Teleconnections?, Science, 301, 1336–1337 doi:10.1126/science.1088626, 2003. 289
Solanki, S. K., Usoskin, I. G., Kromer, B., Schüssler, M., and Beer, J.: Unusual activity of the Sun during recent decades compared to the previous 11 000 years, Nature, 431, 1084, doi:10.1038/nature02995, 2004. 318
Sperling, M., Schmiedl, G., Hemleben, C., Emeis, K. C., Erlenkeuser, H., and Grootes, P. M.: Black Sea impact on the formation of eastern Mediterranean sapropel S1? Evidence from

the Marmara Sea, Science, 190, 9–21, 2003. 318
Stager, J., Cumming, B., and Meeker, L.: A 10 000 year high-resolution diatom record from Pilkington Bay, Lake Victoria, East Africa, Quatern. Res., 59, 172–181, 2003. 318
Stanley, S. and Deckker, P. D.: A Holocene record of allochthonous, aeolian mineral grains in an Australian alpine lake; implications for the history of climate change in southeastern Australia, J. Paleolimnology, 27, 207–219, 2002a. 319
Stanley, S. and Deckker, P. D.: A Holocene record of allochthonous, aeolian mineral grains in an Australian alpine lake; implications for the history of climate change in southeastern Australia, J. Paleolimnol., 27, 207–219, 2002b. 316
Steig, E. J.: Mid-Holocene Climate Change, Science, 286, 1485–1487, 1999. 289, 292
Steig, E. J., Brook, E. J., White, J. W. C., Sucher, C. M., Bender, M. L., Lehman, S. J., Morse, D. L., Waddington, E. D., and Clow, G. D.: Synchronous Climate Changes in Antarctica and the North Atlantic, Science, 282, 92, doi:10.1126/sience.282.5386.92, 1998. 319
Stocker, T., Wright, D., and Broecker, W.: The influence of high-latitude surface forcing on the global thermohaline circulation, Paleoceanography, 7, 529–541, 1992. 298
Stott, L., Cannariato, K., Thunell, R., Haug, G. H., Koutavas, A., and Lund, S.: Decline of surface temperature and salinity in the western tropical Pacific Ocean in the Holocene epoch, Nature, 431, 56–59, 2004. 319
Stuiver, M., Reimer, P. J., Bard, E., Beck, J. W., Burr, G. S., Hughen, K. A., Kromer, B., McCormac, G., van der Plicht, J., and Spurk, M.: INTCAL98 radiocarbon age calibration, 24 000–0 cal BP, Radiocarbon, 40, 1041–1083, 1998. 318
Sun, Y., Oppo, D., Xiang, R., Liu, W., and Gao, S.: Last deglaciation in the Okinawa Trough: Subtropical northwest Pacific link to Northern Hemisphere and tropical climate, Palaeooceanography, 20, 4005, doi:10.1029/2004PA001061, 2005. 319
Te Raa, L. and Dijkstra, H.: Modes of internal thermohaline variability in a single-hemispheric ocean basin, J. Mar. Res., 61, 491–516, 2003. 296, 300
Thompson, L. G., Mosley-Thompson, E., Davis, M. E., Henderson, K. A., Brecher, H. H., Zagorodnov, V. S., Mashiotta, T. A., Lin, P.-N., Mikhalenko, V. N., Hardy, D. R., and Beer, J.: Kilimanjaro ice core records: Evidence of Holocene climate change in tropical Africa, Science, 298, 589–593, 2002. 319
Thompson, L. G., Mosley-Thompson, E., Davis, M., Henderson, P.-N. L. K., Mashiotta, T. A., et al.: Tropical glacier and ice core evidence of climate change on annual to millennial time scales, Clim. Change, 59, 137–155, 2003a. 318

Thompson, L. G., Mosley-Thompson, E., Davis, M., Henderson, P.-N. L. K., Mashiotta, T. A., et al.: Tropical glacier and ice core evidence of climate change on annual to millennial time scales, Clim. Change, 59, 137–155, 2003b. 290, 321
Thomson, D.: Time Series Analysis of Holocene Climate Data, Philosophical Transactions of the Royal Society of London. Series A, Mathematical and Physical Sciences (1934–1990), 330, 601–616, 1990. 292
von Grafenstein, U., Erlenkeuser, H., Müller, J., Jouzel, J., and Johnsen, S.: The cold event 8200 years ago documented in oxygen isotope records of precipitation in Europe and Greenland, Clim. Dynam., 14, 73–81, 1998. 318
von Storch, H., Zorita, E., Jones, J. M., Dimitriev, Y., Gonzalez-Rouco, F., and Tett, S. F. B.: Reconstructing Past Climate from Noisy Data, Science, 306, 679–682, 2004. 289
Wang, E. A.: Millennial reoccurrence of century-scale abrupt events of East Asian Monsoon: a possible heat conveyor for the global deglaciation, Palaeooceanography, 14, 725–731, 1999. 319
Wang, L., Sarnthein, M., Erlenkeuser, H., Grimalt, J., Grootes, P., Heilig, S., Ivanova, E., Kienast, M., Pelejero, C., and Pflaumann, U.: East Asian monsoon climate during the late Pleistocene: high-resolution sediment records from the South China Sea, Mar. Geol., 156, 245–284, 1999. 319
Wang, Y., Cheng, H., Edwards, R., He, Y., Kong, X., An, Z., Wu, J., Kelly, M., Dykoski, C., and Li, X.: The holocene asian monsoon: Links to solar changes and north Atlantic climate, Science, 308, 854–857, 2005. 319
Weber, S. L., Crowley, T. J., and van der Schrier, G.: Solar irradiance forcing of centennial climate variability during the Holocene, Clim. Dynam., 22, 539–553, 2004. 296, 300
Weijer, W. and Dijkstra, H.: Multiple oscillatory modes of the global ocean circulation, J. Phys. Oceanography, 33, 2197–2213, 2003. 296, 298, 300
Wick, L., Lemcke, G., and Sturm, M.: Evidence of lateglacial and Holocene climatic change and human impact in eastern Anatolia: high-resolution pollen, charcoal, isotopic and geochemical records from the laminated sediments of Lake Van, Turkey, 665–675, 2003a. 318
Wick, L., Lemcke, G., and Sturm, M.: Evidence of lateglacial and Holocene climatic change and human impact in eastern Anatolia: high-resolution pollen, charcoal, isotopic and geochemical records from the laminated sediments of Lake Van, Turkey, The Holocene, 13, 665–675, 2003b. 316
Wirtz, K. and Lemmen, C.: A Global Dynamic Model for the Neolithic Transition, Clim. Change,

59, 333–367, 2003. 301
Xiao, J., Nakamura, T., Lu, H., and Zhang, G.: Holocene climate changes over the desert/loess transition of north-central China, Earth and Planet. Sci. Lett., 197, 11–18, 2002. 319
Yu, Z., Vitt, D., Campbell, I., and Apps, M.: Understanding Holocene peat accumulation pattern of continental fens in western Canada, Can. J. Bot., 81, 267–282, 2003. 318
Yuan, D., Cheng, H., Edwards, R. L., Dykoski, C. A., Kelly, M. J., Zhang, M., et al.: Timing, duration, and transitions of the last interglacial Aasian monsoon, Science, 304, 575, doi:10.1126/sience.1091220, 2004. 319
Zhang, M., Yuan, D., Lin, Y., Qin, J., Bin, L., Cheng, H., and Edwards, R. L.: A 6000-year high-resolution climatic record from a stalagmite in Xiangshui Cave, Guilin, China, Holocene, 14, 697–702, 2004. 319

Table 1. Proxy variables used in this study.

Proxy type	Description
Isotopic oxygen fractionation δ^{18}O	The interpretation of isotopic fractionation of oxygen (δ^{18}O) highly depends on geographic location, environmental setting, and type of record. δ^{18}O variations in Andean glaciers and polar ice caps represent temperature. Measured in biologic deposits from closed water bodies, δ^{18}O usually indicates changes in the water balance, and thus effective moisture. However, the signal cannot be separated from temperature effects during times when the lake system is open. Speleothem δ^{18}O records the amount and composition of cave water, mostly during the wet season, and may also be influenced by temperature and above-cave lithology.
Lithic composition Mg/Ca, Charcoal, Clay, Bulk dens., Lightness, Grayscale, HSG, Lithic grains, GSD, LOI	The ratio between Mg and Ca relates to salinity (from calcium precipitation and Mg dissolution) or inorganic material input (magnesium from weathering). Wick et al. (2003b) interpret the variable Mg at constant Ca in a closed lake as changes in effective moisture, similar to the Sr/Ca ratio in ostracod shells (Ricketts et al., 2001). Grayscale density (GSD) and loss on ignition (LOI) quantify the inflow of inorganic versus organic matter. From this, cold/humid and warm/dry climates can identified but the temperature signal not separated from precipitation. The shape of grains indicates the transport process: rounded quartz grains with frequent silica coating point to aeolian import pointing to dry phases in the origin region (Stanley and Deckker, 2002b). Coarse sediment layer with low organic content and many terrestrial plant macrofossils have been used by Noren et al. (2002b) to find exceptional runoff events and thus storminess. Occurence of allochtonous hematite-stained grains (HSG) and icelandic glass points to ice-rafting as a consequence of increased glacier calving (e.g. Bond et al., 2001c); The preservation status of aragonite at intermediate measures the bottom-water corrosiveness, and is therefore indicative for changes in the THC.

Table 1. Continued.

Proxy type	Description
Species composition Pollen, Radiolaria, % Diatoms	Relative abundance of algal species is related to stratification and mixed layer depth and, thus, to the factor controlling both variables such as trade wind strength or freshwater increase. Pollen spectra are often taken to infer precipitation anomalies (as shaping the community structure within forests).

Table 2. Location, type, temporal coverage and reference of the climate proxy time series used in this study; the numbers in the table identify the position of proxy sites in the map (Fig. 1). Abbreviations: SS=sea surface, T=temperature, S=salinity, P=precipitation, LG=lithic grains, SSN=sun spot number, Lk=Lake, Cv=Cave.

No	Site	Proxy	Per	Reference	No	Site	Proxy	Per	Reference
1	NW Alaska	Mg/Ca T	0–11	Hu et al. 1998	2	NW Pacific	$\delta^{18}O$	0–12	Oba and Murayama 2004
3	Owens Lk, CA	$\delta^{18}O$	0–12	Benson et al. 2002	4	E California	P	0–8	Hughes and Graumlich 1996
5	W Canada	Density	0–8	Yu et al. 2003	6	S California	Moisture	0–7	Davis 1992
7	Moon Lk, ND	Salinity	0–11	Laird et al. 1996	8	Kimble, MN	Charcoal	0–12	Camill et al. 2003
9	Sharkey, MN	Charcoal	0–12	Camill et al. 2003	10	NC America	$\delta^{18}O$	0–9	Denniston et al. 1999
11	Cold Water Cv, IA	$\delta^{18}O$	0–8	Dorale et al. 1992	12	Guatemala	$\delta^{18}O$ (Cy)	0–8	Curtis et al. 1998
13	Guatemala	$\delta^{18}O$ (Co)	0–10	Curtis et al. 1998	14	Guatemala	$\delta^{18}O$ (Py)	0–10	Curtis et al. 1998
15	E Pacific	$\delta^{18}O$	2–12	Rosenthal et al. 2003	16	Yucatan	$\delta^{18}O$ (Ph)	0–8	Hodell et al. 1995
17	Yucatan	$\delta^{18}O$ (Py)	0–8	Hodell et al. 1995	18	Costa Rica	$\delta^{18}O$	5–9	Lachniet et al. 2004
19	E Canada	Charcoal	0–7	Carcaillet et al. 2001	20	Ecuador	ENSO	0–10	Moy et al. 2002
21	E Canada	Charcoal	0–8	Carcaillet et al. 2001	22	Ecuador	GSD	0–12	Rodbell et al. 1999
23	Huascaran, Peru	$\delta^{18}O$	0–12	Thompson et al. 2003a	24	Chile	$\delta^{18}O$	0–8	Lamy et al. 2002
25	Chilean Coast	SST	0–8	Lamy et al. 2001	26	Haiti	$\delta^{18}O$	0–10	Higuera-Gundy et al. 1999
27	New England	Storms	0–12	Noren et al. 2002a	28	Lk Titikaka	Level	0–4	Abbott et al. 1997
29	Sajama, Bolivia	Particles	0–12	Thompson et al. 2003a	30	Sajama, Bolivia	$\delta^{18}O$	0–12	Thompson et al. 2003a
31	Venezuela	$\delta^{18}O$	0–8	Curtis et al. 1999	32	NE Canada	GSD	4–9	Barber et al. 1999
33	W Antarctic	Inclination	1–9	Brachfeld et al. 2000	34	Cariaco Basin	GSD	0–12	Haug et al. 2001
35	Cariaco Basin	Titanium	0–12	Haug et al. 2001	36	Cariaco Basin	SST	0–12	Lea et al. 2003
37	Bermuda Rise	$\delta^{18}O$	1–10	Keigwin 1996	38	Botuvera Cv, Brasil	$\delta^{18}O$	0–12	Cruz et al. 2005
39	Greenland Ice	Be^{10}	3–12	Finkel and Nishiizumi 1997	40	Greenland Ice	$\delta^{18}O$	0–10	Grootes and Stuiver 1997
41	Greenland Ice	SSN	0–11	Solanki et al. 2004	42	Greenland Ice	$\delta^{14}C$	0–12	Stuiver et al. 1998
43	W Atlantic	$\delta^{18}O$ (Tu)	0–11	Arz et al. 2001	44	W Atlantic	$\delta^{18}O$	0–11	Arz et al. 2001
45	Eq Atlantic	ΔSST	0–12	Kim and Schneider 2003	46	N Atlantic	HSG	0–12	Gupta et al. 2003
47	N Atlantic	LG	1–12	Bond et al. 1997a	48	Trop Atlantic	$\delta^{18}O$	0–11	Knaack 1997
49	Trop Atlantic	SST	0–12	deMenocal et al. 2000a	50	N Atlantic	HSG	0–12	Bond et al. 2001a
51	Canary	$\delta^{18}O$	0–12	Freudenthal et al. 2002	52	Ireland	$\delta^{18}O$	0–10	McDermott 2004
53	NW Morocco	$\delta^{18}O$	5–9	Hodell et al. 2001a	54	SW Europe	ΔT	0–12	Davis et al. 2003a
55	NW Europe	ΔT	0–12	Davis et al. 2003a	56	S Atlantic	LG	0–10	Hodell et al. 2001b
57	Swiss Alpes	T7	0–9	Wick et al. 2003a	58	Swiss Alpes	P	0–9	Wick et al. 2003a
59	Swiss Alpes	P	0–8	Wick et al. 2003a	60	C Italy	Mg/Ca T	1–7	Drysdale et al. 2006
61	Angola Basin	$U^{k'}_{37}$ SST	0–12	Kim and Schneider 2003	62	C Italy	$\delta^{18}O$	1–7	Drysdale et al. 2006
63	S Germany	$\delta^{18}O$	0–12	von Grafenstein et al. 1998	64	Sahel	$\delta^{18}O$	0–12	Gasse 2002
65	N Atlantic	SST	1–12	Sarnthein et al. 2003a	66	N Norway	T	1–8	Husum and Hald 2004
67	Sweden	GSD	1–11	Rubensdotter and Rosqvist 2003	68	N Finland	T	1–8	Husum and Hald 2004
69	N Atlantic	GSD	1–12	Chapman et al. 2000	70	Marmara Sea	$\delta^{18}O$	0–12	Sperling et al. 2003
71	Marmara Sea	$U^{k'}_{37}$ SST	0–12	Sperling et al. 2003	72	SE Africa	$\delta^{18}O$	0–10	Holmgren et al. 2003
73	Burundi	P	0–12	Bonnefille and Chalie 2000	74	Black Sea	Ti	1–12	Bahr et al. 2005
75	SE Europe	ΔT	0–12	Davis et al. 2003a	76	Kola	$\delta^{18}O$	0–9	Jones et al. 2004
77	Lk Victoria	Diatoms	0–10	Stager et al. 2003	78	Lk Malawi	Si	0–12	Johnson et al. 2002
79	Lk Malawi	MAR	0–12	Johnson et al. 2002	80	SE Mediterranean	$\delta^{18}O$	0–4	Schilman et al. 2003
81	SE Mediterranean	$\delta^{18}O$	0–4	Schilman et al. 2003	82	Soreq Cv, Israel	$\delta^{18}O$	0–12	Bar-Matthews et al. 1999
83	Red Sea	$\delta^{18}O$	1–12	Seeberg-Elverfeldt et al. 2004	84	Lk Sim, Kenia	$\delta^{18}O$	1–10	Barker et al. 2001

Table 2. Continued.

No	Site	Proxy	Per	Reference	No	Site	Proxy	Per	Reference
85	Lk Hall, Kenia	$\delta^{18}O$	1–12	Barker et al. 2001	86	Kilimanjaro	$\delta^{18}O$	0–12	Thompson et al. 2002
87	Lk Abhe, Ethiopia	Level	0–10	Gasse 2000	88	Somalia	$\delta^{18}O$	0–10	Jung et al. 2004
89	Qunf Cv, Oman	$\delta^{18}O$	0–11	Fleitmann et al. 2007	90	Oman	$\delta^{18}O$	3–8	Fleitmann et al. 2003
91	Arabian Sea	$\delta^{18}O$	0–11	Gupta et al. 2003	92	Arabian Sea	SSTW	0–12	Schulz 1995
93	NE Arabian Sea	$\delta^{18}O$	0–12	Doose-Rolinski et al. 2001	94	NW Siberia	T7	0–4	Hantemirov and Shiyatov 2002
95	E Arabian Sea	$\delta^{18}O$	0–10	Sarkar et al. 2000	96	Lk Issyk-Kul, Kyrgyzstan	$\delta^{18}O$	3–9	Ricketts et al. 2001
97	Tibet	$\delta^{18}O$	0–12	Fontes et al. 1996	98	Dunde, China	$\delta^{18}O$	0–9	Jung et al. 2004
99	Komsomolskaia	$\delta^{2}H$	0–12	Masson et al. 2000	100	N Siberia	Pollen	0–11	Andreev et al. 2003
101	NW China	P (AC)	2–11	Herzschuh et al. 2004	102	NW China	P (Ef)	2–11	Herzschuh et al. 2004
103	Dongge Cv, China	$\delta^{18}O$	0–9	Wang et al. 2005	104	Vostok, Antarctica	$\delta^{2}H$	0–12	Petit et al. 1999
105	N China	Clay	0–10	Xiao et al. 2002	106	S China	Moisture	0–10	Liu et al. 2000a
107	Xiangshui Cv, China	$\delta^{18}O$	0–6	Zhang et al. 2004	108	S China Sea	$\delta^{18}O$	3–12	Kienast et al. 2001
109	N China	GSD	5–10	Jin et al. 2004	110	S China Sea	$\delta^{18}O$	0–12	Wang et al. 1999
111	Taiwan	LOI	2–12	Huang et al. 1997	112	S China Sea	SSS	0–9	Jung et al. 2004
113	S China Sea	$\delta^{18}O$	0–11	Wang et al. 1999	114	S China Sea	Silt	0–12	Wang et al. 1999
115	S China Sea	$\delta^{18}O$	0–12	Wang 1999	116	Dongge Cv, China	$\delta^{18}O$	0–12	Yuan et al. 2004
117	Sulu Sea	$\delta^{18}O$	4–12	Rosenthal et al. 2003	118	W Pacific	$\delta^{18}O$ (81)	0–12	Stott et al. 2004
119	E China Sea	SST	1–12	Sun et al. 2005	120	E China Sea	SST	0–11	Fengming et al. 2008
121	W Pacific	$\delta^{18}O$	0–12	Rosenthal et al. 2003	122	W Pacific	$\delta^{18}O$ (76)	0–12	Stott et al. 2004
123	NW Pacific	%Nitzschia	0–7	Shimada et al. 2004	124	NW Pacific	%Ozeanica	0–7	Shimada et al. 2004
125	S Australia	T	0–4	Cook et al. 2000	126	Tasmania	T	0–4	Cook et al. 2000
127	Tasmania	T	0–4	Cook et al. 2000	128	SW Australia	Particles	1–12	Stanley and Deckker 2002a
129	Taylor dome	$\delta^{18}O$	0–12	Grootes et al. 1994	130	Taylor dome	$\delta^{2}H$	0–12	Steig et al. 1998

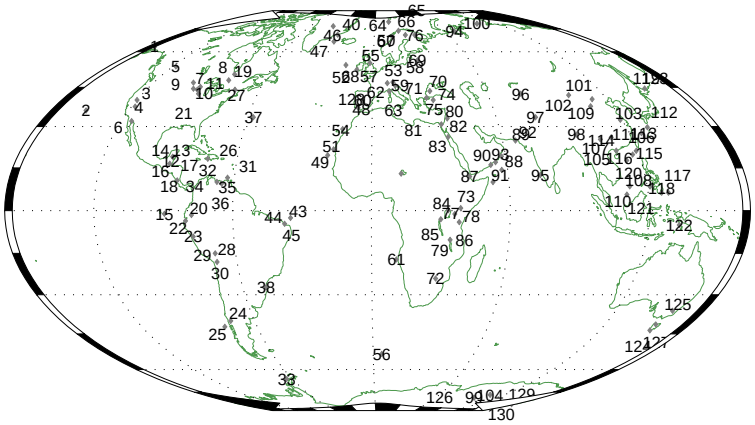

Fig. 1. Global distribution of high-resolution proxy time series used in this study. Numbers of the 130 records (109 sites) refer to Table 2.

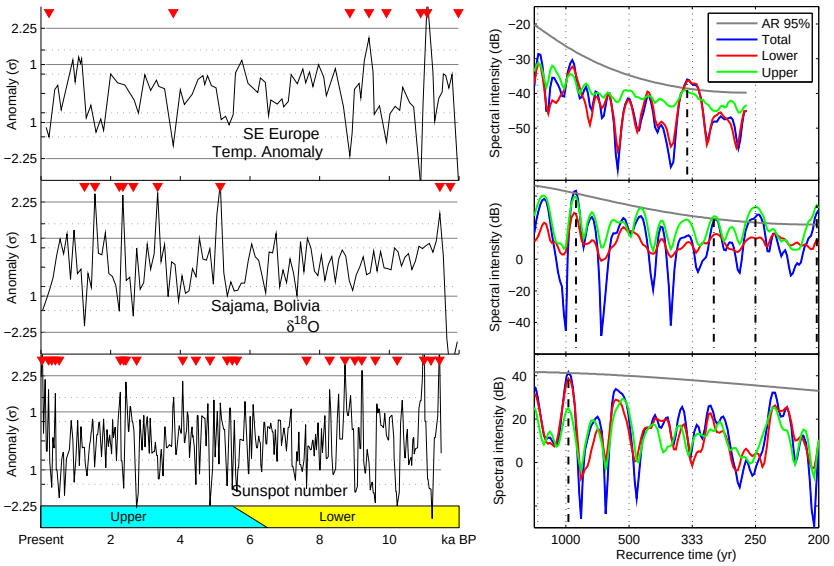

Fig. 2. Three selected records: Temperature reconstruction for Southeast Europe, (Davis et al., 2003b), isotopic oxygen at Sajama, Bolivia (Thompson et al., 2003b) and sunspot number from Greenland ice cores (**?**). Left: De-trended and normalized data. Non-cyclic events according our definition with p_a=1.5 are marked with red triangles. Right: Spectral amplitudes after applying the Lomb-Scargle transformation (black: total record, red: bootstrapping of upper interval, thus indicating periodicity confined to the Lower Holocene, green: Upper Holocene spectrum). Dashed lines indicate significant frequencies.

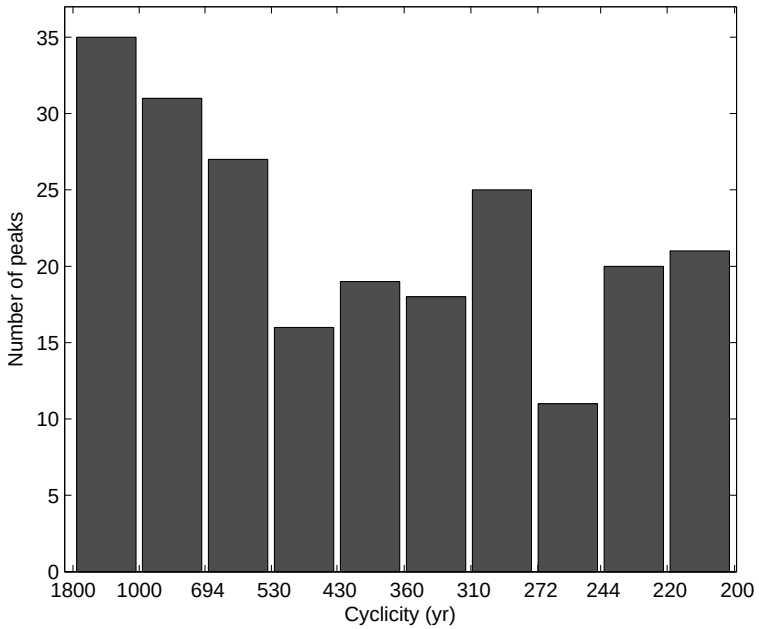

Fig. 3. Histogram of dominant modes in all 130 records.

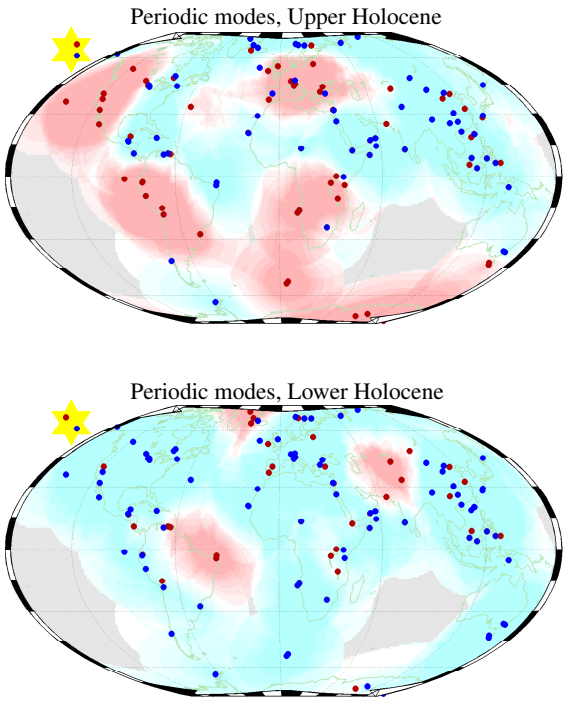

Fig. 4. Sites with significant periodicity (red, without: blue) in the Upper and Lower Holocene. For spatial extrapolation see Methods, results for proxies related to solar activity are displayed in the yellow polygon.

323

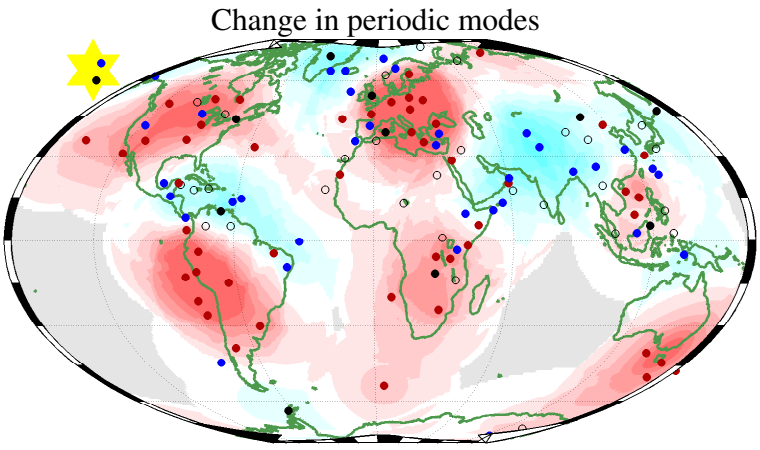

Fig. 5. Change in periodic fluctuations from the Lower to the Upper Holocene (positive change: red, negative: blue, no significance: empty circle, significant mode without change: filled black).

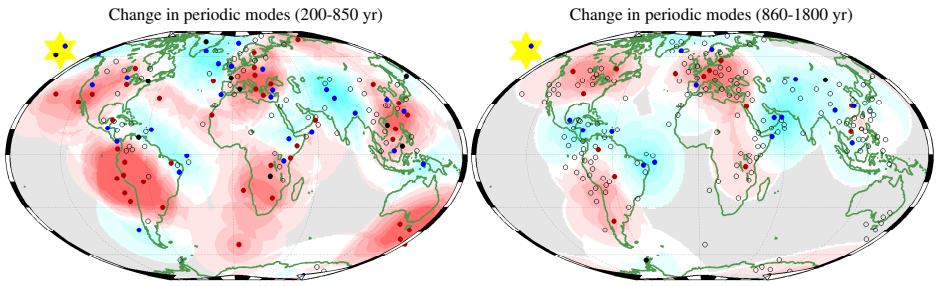

Fig. 6. Change in periodic fluctuations from the Lower to the Upper Holocene separated according spectral interval (for symbols, see Fig. 5).

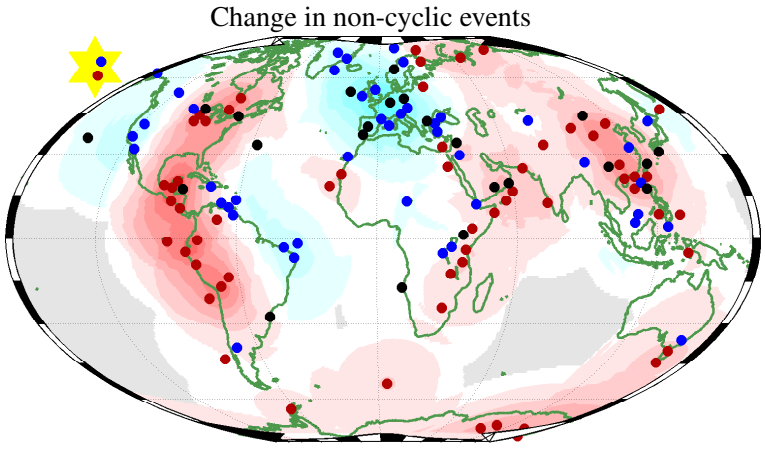

Fig. 7. Negative and positive Mid-Holocene change in non-cyclic frequency (number of events per millennium). Red areas collect sites where non-cyclic frequency increased by more than 0.1 events kyr^{-1} more in the Upper compared to the Lower Holocene. In blue areas, anomaly frequency decreases by more than 0.1 events kyr^{-1}.